

# Influence of threshold effects induced by $P$ -wave charmed mesons

Xiao-Hai Liu<sup>1\*</sup>

<sup>1</sup> *Department of Physics and State Key Laboratory of Nuclear Physics and Technology,  
Peking University, Beijing 100871, China*

March 13, 2014

## Abstract

We investigate the processes  $e^+e^-$  annihilating to  $J/\psi\pi\pi$ ,  $\psi'\pi\pi$  and  $h_c\pi\pi$ . The coupled-channel effects induced by the couplings between the widely accepted  $D$ -wave charmonia  $\psi(4160)$  and  $D_1D$ ,  $D_1D^*$  and  $D_2D^*$  charmed meson pairs are highlighted, taking into account these couplings are  $S$ -wave, and will respect heavy quark spin symmetry. The lineshapes show some non-trivial cusps which result from the singularities of the rescattering loops, which could be helpful in understanding the nature of  $Y(4260)$ ,  $Y(4360)$ ,  $Z_c(3900)/Z_c(3885)$  and  $Z_c(4020)/Z_c(4025)$ .

PACS: 13.25.Gv, 14.40.Pq, 13.75.Lb

---

\*E-mail address: liuxiaohai@pku.edu.cn

# 1 Introduction

There has been a renewal of QCD spectroscopy in the last decade, initiated by the findings of numerous  $XYZ$  states near the open-flavor thresholds. Most of these states do not fit into the predictions of the quenched potential quark model, which has been proved to be very successful in describing the conventional heavy quarkonia below open-flavor threshold. These inconsistencies remind people that the vacuum polarization effect of dynamical fermions should receive more attention in understanding the heavy quarkonium spectroscopy. This vacuum polarization effect could be compensated by the coupled-channel effects induced by the coupling between heavy quarkonia and open-flavor mesons. After taking into account the coupled-channel effects, the mass and decay properties of the heavy quarkonia will be changed significantly, especially when the mass of the heavy quarkonia are close to the corresponding open-flavor threshold (see Refs. [1, 2, 3, 4, 5, 6, 7]).

The mysterious charmonium-like state  $Y(4260)$  has many peculiar characteristics. As a charmonium candidate, it is observed in the  $J/\psi\pi\pi$  channel, but not in the open charm decay channels which are supposed to be favorable decay modes of conventional  $c\bar{c}$  states. The  $R$ -value scan around 4.26 GeV also appears to have a dip instead of a bump structure. The state observed in  $\psi'\pi\pi$  channel,  $Y(4360)$ , has similar puzzles as those of  $Y(4260)$ . Recent experimental observations revive discussions on the nature of  $Y(4260)$ . Several charged charmonium-like structures,  $Z_c(3900)$ ,  $Z_c(3885)$ ,  $Z_c(4020)$  and  $Z_c(4025)$ , are observed while studying  $Y(4260)$  [8, 9, 10, 11, 12, 13], which makes  $Y(4260)$  become more intriguing. We refer to Refs. [14, 15] for a recent review.

The influence of the coupled-channel effects on charmonia induced by  $P$ -wave charmed mesons has not been widely studied before because of their relatively larger masses. On the other hand, the thresholds of the combinations of  $S$ - and  $P$ -wave charmed mesons are very close to  $Y(4260)$  and  $Y(4360)$ , and their couplings with the parity-odd charmonia could be  $S$ -wave, which is supposed to be strong. In this work, we will study the influence of the coupled-channel effects on the lineshapes of some pertinent cross sections and invariant mass distributions, where the contributions from  $P$ -wave charmed mesons are highlighted.

# 2 The model

We will build our model within the framework of heavy hadron chiral perturbation theory (HHChPT). In HHChPT, to encode the heavy quark spin symmetry (HQSS), the doublets with light degrees of freedom  $J^P = 1/2^-, 1/2^+, 3/2^+$  are collected into three superfields

$$H_a = \frac{1 + \not{v}}{2} [\mathcal{D}_{a\mu}^* \gamma^\mu - \mathcal{D}_a \gamma_5], \quad (1)$$

$$S_a = \frac{1 + \not{v}}{2} [\mathcal{D}_{1a}^{\prime\mu} \gamma_\mu \gamma_5 - \mathcal{D}_{0a}^*], \quad (2)$$

$$T_a^\mu = \frac{1 + \not{v}}{2} \left\{ \mathcal{D}_{2a}^{\mu\nu} \gamma_\nu - \sqrt{\frac{3}{2}} \mathcal{D}_{1a\nu} \gamma_5 \left[ g^{\mu\nu} - \frac{1}{3} \gamma^\nu (\gamma^\mu - v^\mu) \right] \right\}, \quad (3)$$

respectively, where  $a$  is the light flavor index. For clarity, in what follows, we will use  $HH$  to represent the  $D^{(*)}D^{(*)}$  combinations, with the similar conventions for  $TH$  and  $SH$ . The  $S$ -wave charmonia  $\psi(nS)$  may couple to  $HH$  and  $SH$  via relative  $P$ - and  $S$ -wave respectively, where  $n$  denotes the radial quantum number. Required by HQSS, the total angular momentum of the light degrees of freedom

should also be conserved for these couplings. For  $TH$  combinations, the light degrees of freedom carry angular momentum  $3/2$  and  $1/2$  respectively, in an  $S$ -wave they cannot produce 0 angular momentum carried by the light degrees of freedom of  $\psi(nS)$ . As a result, the  $S$ -wave coupling between  $\psi(nS)$  and  $TH$ , although allowed by the parity conservation, will be suppressed according to HQSS, as discussed in Ref. [16]. In the heavy quark limit, the only allowed coupling is  $D$ -wave. However, for the coupling between  $D$ -wave charmonia  $\psi(nD)$  and  $TH$ , the  $S$ -wave is allowed, since its light degrees of freedom is 2. This gives us a hint that the coupled-channel interactions between  $\psi(nD)$  and  $TH$  may largely affect the mass and decay properties of  $\psi(nD)$ , especially for the  $D$ -wave charmonia close to the  $TH$  thresholds. In charmonium family,  $\psi(4160)$  is widely considered as a conventional  $2^3D_1$  charmonia, with its mass and width are estimated by PDG to be  $M_\psi=4153 \pm 3$  MeV and  $\Gamma_\psi=103 \pm 8$  MeV [17]. If using the latest data, its mass and width are found to be  $M_\psi=4191.7 \pm 6.5$  MeV and  $\Gamma_\psi=71.8 \pm 12.3$  MeV in Ref. [18], or  $M_\psi=4193 \pm 7$  MeV and  $\Gamma_\psi=79 \pm 14$  MeV in Ref. [19], which are very close to the  $TH$  thresholds and the mass of  $Y(4260)$ . Therefore it is natural to wonder whether there is some kind of connection between these states and the  $TH$  coupled-channels. For further discussion, we mention that  $HH$  may couple to  $\psi(nD)$  via  $P$ -wave, and the  $S$ -wave coupling between  $SH$  and  $\psi(nD)$  is also suppressed according to HQSS.  $SH$  may couple to  $\psi(nS)$  via  $S$ -wave.

There are plenty of data for  $e^+e^-$  annihilating to one heavy quarkonium plus two pion mesons. Many interesting phenomena have been discovered in these channels. We will investigate these exclusive processes in this work to try to quantify the coupled-channel effects. Taking into account the previous discussions, using HHChPT power counting we introduce the leading order effective Lagrangian as follows:

$$\begin{aligned}
\mathcal{L}_1 = & \frac{g_T}{\sqrt{2}} \langle J^{\mu\nu} \bar{H}_a^\dagger \gamma_\nu \bar{T}_{a\mu} - J^{\mu\nu} \bar{T}_{a\mu}^\dagger \gamma_\nu \bar{H}_a \rangle \\
& + ig_H \langle J^{\mu\nu} \bar{H}_a^\dagger \gamma_\mu \overleftrightarrow{\partial}_\nu \bar{H}_a \rangle \\
& + g_S \langle J \bar{S}_a^\dagger \bar{H}_a + J \bar{H}_a^\dagger \bar{S}_a \rangle \\
& + C_S \langle J \bar{H}_b^\dagger \gamma_\mu \gamma_5 \bar{H}_a \mathcal{A}_{ba}^\mu \rangle \\
& + iC_P \langle J^\mu \bar{H}_b^\dagger \sigma_{\mu\nu} \gamma_5 \bar{H}_a \mathcal{A}_{ba}^\nu \rangle + h.c.,
\end{aligned} \tag{4}$$

where  $\langle \dots \rangle$  means the trace over Dirac matrices,  $\mathcal{A}^\mu$  is the chiral axial vector containing the Goldstone bosons, and the fields for the  $S$ -,  $P$ - and  $D$ -wave charmonia read

$$\begin{aligned}
J = & \frac{1+\not{v}}{2} [\psi(nS)^\mu \gamma_\mu] \frac{1-\not{v}}{2}, J^\mu = \frac{1+\not{v}}{2} [h_c(nP)^\mu \gamma_5] \frac{1-\not{v}}{2} \\
J^{\mu\nu} = & \frac{1+\not{v}}{2} \left\{ \psi(nD)_\alpha \left[ \frac{1}{2} \sqrt{\frac{3}{5}} [(\gamma^\mu - v^\mu) g^{\alpha\nu} \right. \right. \\
& \left. \left. + (\gamma^\nu - v^\nu) g^{\alpha\mu}] - \sqrt{\frac{1}{15}} (g^{\mu\nu} - v^\mu v^\nu) \gamma^\alpha \right] \right\} \frac{1-\not{v}}{2},
\end{aligned} \tag{5}$$

respectively, where only the states relevant for our discussion are included. The effective Lagrangian for the strong interactions of heavy mesons with Goldstone bosons reads

$$\begin{aligned}
\mathcal{L}_2 = & i \frac{h'}{\Lambda_\chi} \langle \bar{H}_a T_b^\mu \gamma^\nu \gamma_5 (D_\mu \mathcal{A}_\nu + D_\nu \mathcal{A}_\mu)_{ba} \rangle \\
& + ih \langle \bar{H}_a S_b \gamma_\mu \gamma_5 \mathcal{A}_{ba}^\mu \rangle + ig \langle H_b \gamma_\mu \gamma_5 \mathcal{A}_{ba}^\mu \bar{H}_a \rangle.
\end{aligned} \tag{6}$$

Some of these Lagrangians have been introduced in Refs. [20, 21, 22, 23, 24, 25], we refer to Ref. [21] for a review and some conventions.

The coefficient  $g_T$  in Eq. (4), which describes the coupling strength between  $\psi(nD)$  and  $TH$ , is not well determined. But taking into account the coupling is  $S$ -wave, it may be expected to be large. There are some indirect experimental evidences to support this argument. For instance,  $\psi(4415)$  is a widely accepted  $S$ -wave charmonia, its decaying to  $D_2D$  is  $D$ -wave decay, but the branching fraction is very large, which is  $(10 \pm 4)\%$  estimated by PDG [17]. Therefore it seems to be reasonable to expect the  $S$ -wave coupling constant  $g_T$  could also be sizeable. Of course this is not a serious estimation, to obtain some less model dependent result, we will only focus on the lineshape behavior of the total and differential cross sections of the pertinent channels in this work.

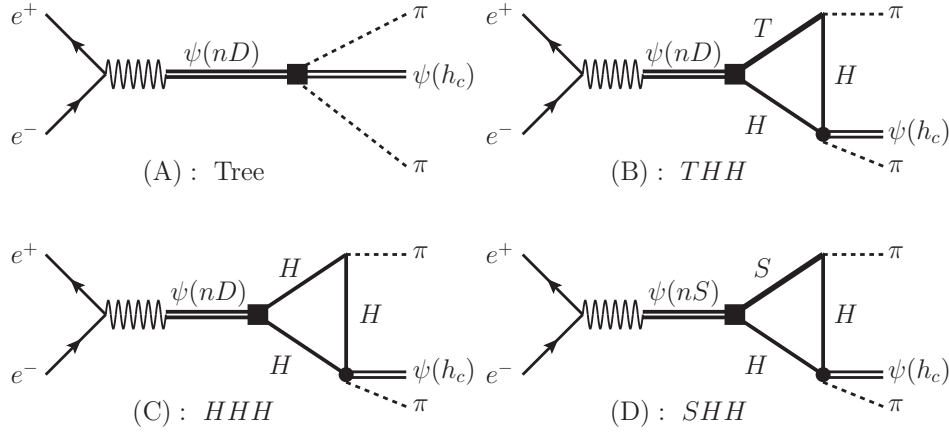


Figure 1: Feynman diagrams for the dipion transitions.

The Feynman diagrams which contribute to the dipion transitions are displayed in Fig. 1, where we will take  $\psi(4160)$  as the most relevant  $\psi(nD)$  state, and use its PDG averaged mass and width as the input parameters in our calculation. Although the production of the  $D$ -wave charmonia in  $e^+e^-$  annihilation is supposed to be suppressed, the experimental data indicates the electron decay width of  $\psi(4160)$  is not small, i.e.  $\Gamma_{ee} = (0.83 \pm 0.07) \text{ KeV}$  [17], which possibly results from  $S$ - $D$  mixing effect. However, we still face a dilemma here. The larger electron decay width of  $\psi(4160)$  implies the HQSS breaking effects, or some higher order contributions in the effective theory, may also be important, which is mainly due to the charm quark is not so heavy. For the moment we will ignore some symmetry breaking effects, such as the breaking in the couplings between  $\psi(nD)$  and  $TH$ , and still follow the guidance of HQSS (see Refs. [16, 26] for some discussions on the symmetry breaking effects).

Fig. 1(A) indicates the tree diagram contribution, and the amplitude will be proportional to a Breit-Wigner form function

$$BW[\psi(4160)] = (s - M_\psi^2 + iM_\psi\Gamma_\psi)^{-1}, \quad (7)$$

where  $s$  is the center of mass energy squared. The cross section lineshape of this diagram will be trivial, which is just the usual Breit-Wigner structure, but it can provide some background that may affect the lineshape behavior via interference.

Concerning Fig. 1(B), named as  $THH$  loop in this work, there are four sub diagrams categorized by the intermediated charmed mesons:

$$\text{I) } \{D_1D [D^*]\},$$

- II)  $\{D_1 D^* [D^*]\}$ ,
- III)  $\{D_2 D^* [D]\}$ ,
- IV)  $\{D_2 D^* [D^*]\}$ ,

where the charmed mesons in the brackets correspond to the vertical propagators in the  $THH$  loops. Concerning these triangle loops which describe the coupled-channel effects, in some special kinematic configurations, all of the three intermediate states can be on-shell simultaneously. This is the so called triangle singularity (TS) or "two cut" condition [27, 28, 29, 30, 31]. Since this kind of singularities usually appears when the mass of the external particle is very close to the threshold of intermediate states, it may change the threshold behavior dramatically and show up directly as a bump or cusp in the amplitude. The  $THH$  loops just approximately meet the kinematic conditions of this special singularity. For  $J/\psi(\psi')\pi\pi$  final states, the amplitudes corresponding to the above four sub diagrams have a simple relation in the heavy quark limit, i.e.,

$$\mathcal{M}^I : \mathcal{M}^{II} : \mathcal{M}^{III} : \mathcal{M}^{IV} = 1 : \frac{1}{2} : -\frac{1}{5} : \frac{3}{10} . \quad (8)$$

This implies the main contribution may come from  $\{D_1 D [D^*]\}$  loop. For  $\psi(nD) \rightarrow h_c \pi \pi$ , the spin of the charm quark is flipped, which means in the heavy quark limit this process is forbidden. However, since we are using physical mass as input in the calculation and the masses of the charmonia and charmed mesons are not so heavy, the amplitude still could be sizeable. In Fig. 2, we display the lineshapes of the energy dependence of the cross sections for  $e^+e^- \rightarrow J/\psi \pi \pi$ ,  $\psi' \pi \pi$  and  $h_c \pi \pi$  via the  $D$ -wave state  $\psi(4160)$  and  $THH$  loops. For  $J/\psi \pi \pi$  channel, apart from the  $\psi(4160)$  bump, three cusps appeared at the thresholds of  $D_1 D$ ,  $D_1 D^*$  and  $D_2 D^*$  respectively, with  $D_1 D$  cusp is the most obvious one, which can be understood according to Eq. (8). The peak position of  $\psi(4160)$  is upward shifted because of the interference with  $D_1 D$  cusp. For  $\psi' \pi \pi$  and  $h_c \pi \pi$  channels, the  $\psi(4160)$  bump is nearly smeared since the  $D_1 D$  cusp is much stronger. This can be attributed to the thresholds of  $\psi' \pi$  and  $h_c \pi$  are much closer to that of  $HH$ , compared with that of  $J/\psi \pi$ , which will strengthen the TS. There is another way to understand this point. If we assume there are  $Z_c(3900)$  and  $Z_c(4020)$  molecular states produced in this  $THH$  loop mechanism, which corresponds to plug two propagators into the black bubble of the diagram Fig. 1(B) separately, the lineshapes will be changed to some extent, as illustrated in Fig. 2. Taking into account the four types of  $THH$  loops, if we plug in  $Z_c(3900)$ , since it stays in the vicinity of  $DD^*$  threshold,  $\mathcal{M}^I$  will become so strong that the  $D_1 D^*$  and  $D_2 D^*$  cusps blur to obscurity. On the other hand, if we plug in  $Z_c(4020)$  which is much closer to the  $D^* D^*$  threshold,  $\mathcal{M}^{II}$  and  $\mathcal{M}^{IV}$  will be strengthened, therefore the  $D_1 D^*$  and  $D_2 D^*$  cusps turn to be more obvious.

The lineshapes of the differential cross sections also show some nontrivial phenomena. We display the results at several center of mass energy points, as illustrated in Fig. 2. For  $J/\psi \pi$  distribution, there is a mini cusp appeared around  $DD^*$  threshold at  $\sqrt{s} = 4.16$  GeV. With the energy increasing and being close to  $D_1 D$  threshold, the TS may occur and a clear narrow cusp emerged around  $DD^*$  threshold at  $\sqrt{s} = 4.26$  GeV. With the continuous growth of the energy, the contributions of  $\mathcal{M}^{II}$ ,  $\mathcal{M}^{III}$  and  $\mathcal{M}^{IV}$  become more and more significant, and the cusp around  $D^* D^*$  is emerging, but the cusp around  $DD^*$  is fading since the energy is leading away from the favorable region of the TS of  $\mathcal{M}^I$ . For  $\psi' \pi$  and  $h_c \pi$  distributions, the  $D^* D^*$  cusp has already showed up around  $\sqrt{s} = 4.36$  GeV. When the energy comes to 4.415 GeV, the  $D^* D^*$  cusp becomes very obvious. It should be mentioned these cusps are also affected by the reflection effects in the Dalitz plot.

From the above discussions, it can be concluded that the kinematics play a crucial role to produce these lineshapes, both in total and differential cross sections. That is because the TS of the  $THH$  loops has its favorable kinematic region, it is sensitive both to the masses of the internal and external lines, and another important relevant factor is the phase space. These causes lead to the production of different cusps for different final states and different energy points. The  $\psi'\pi\pi$  channel can be taken as a direct prediction to check this argument, since its dynamical production mechanism is the same with that of  $J/\psi\pi\pi$  but the kinematics is different.

If comparing Fig. 2 with the experimental data in Refs. [8, 9, 10, 13, 32], it can be noted that these cusps just fall in the corresponding vicinities of  $Y(4260)$ ,  $Y(4360)$ ,  $Z_c(3900)/Z_c(3885)$  and  $Z_c(4020)/Z_c(4025)$  in the same processes, and there are none genuine resonances introduced in this model. These cusps are generated in the dipion transitions by this special rescattering mechanism, but the open-charm channels,  $D_{(s)}^{(*)}D_{(s)}^{(*)}$ , will not suffer from this mechanism. Therefore it will not be very surprising to observe a dip in  $R$ -value scan and open charm distributions around  $\sqrt{s}=4.26$  GeV and 4.36 GeV. Apart from this, there is  $DD^*$  ( $Z_c(3900)$ ) but no  $D^*D^*(Z_c(4020))$  threshold bump obtained in  $J/\psi\pi$  distribution, which is in agreement with the experimental observations [8, 9]. In  $h_c\pi\pi$  final states, there are a distinct  $Z_c(4020)$  and an obscure  $Z_c(3900)$  observed in experiment, which could also be understood from the above discussions, since the experimental data samples are collected at the center of mass energies from 3.9 to 4.42 GeV [10], correspondingly in our model the favorable production region for  $Z_c(4020)$  and  $Z_c(3900)$  is changing in this range.

However, just according to this simple model, the peak positions and bump structures are not precisely consistent with the current data. For instance, there is still a shifted  $\psi(4160)$  bump appeared in Fig. 2(a), but this structure is not clear in experiment [33]. Another inconsistency is the  $DD^*$  cusps are stronger than  $D^*D^*$  cusps at  $\sqrt{s}=4.26$  GeV and 4.36 GeV in Fig. 2(f)(compared with Ref. [10]), although we concluded that the strength of the cusps are sensitive to energies. To compensate for the deficiency of this simplified scenario, it seems that we need some proper interferences between the trivial diagrams and  $THH$  loops. This seems to be possible, since the trivial diagrams will only affect the energy region around  $M_{\psi(4160)}$  according to the Breit-Wigner function Eq. (7), a proper destructive interference will possibly flatten out the bump around  $\psi(4160)$ . On the other hand, for  $\psi'\pi\pi$  and  $h_c\pi\pi$  final states, as the  $\psi(4160)$  structure is already smeared, the interference may possibly make it show up again and change the  $D_1D$  cusp structure. With the center of mass energy increasing, the contribution from some other higher charmonia, such as  $\psi(4415)$ , will be involved.  $\psi(4415)$  stays close to the thresholds of  $TH$  too, but these couplings are  $D$ -wave, whose contribution will be higher order and the cusps are expected to be waken. If we take into account  $S$ - $D$  mixing between charmonia,  $\psi(4415)$  can also couple to  $TH$  via  $S$ -wave. Since its mass are closer to  $D_1D^*$  compared with  $D_1D$ , it will strengthen  $\mathcal{M}^{II}$  and then strengthen the  $D^*D^*$  cusp. This may also compensate for the deficiency appeared in  $h_c\pi\pi$  channel. However, since we can not give reliable estimations of the pertinent couplings for the moment, these are just some qualitative speculation.

There are also some theoretical uncertainties concerning our scenario. For  $HH\rightarrow J/\psi(\psi')\pi$ , there are two mechanisms that contribute at the same order according to the HHChPT power counting. One is the short distance process mediated by the contact interaction, as we used in our model. Another one is the  $t$ -channel process by exchanging an off shell charmed meson. For  $HH\rightarrow h_c\pi$ , the contribution from the second one is even at a lower order. If we take the  $t$ -channel interaction into account, it will change the triangle diagram to the box diagram. But the singular properties of the box diagram can be ascribed to the triangle diagrams, and the most important contribution still comes from the case when  $THH$  are approximately on shell. To simplify the calculation and highlight the intrinsic characters of the loops, i.e. TS, we will mainly discuss the triangle diagrams here. The relative strength of the



rescattering amplitude will be affected by these theoretical uncertainties, but the singularity behavior of the loops is mainly in connection with the kinematics, and the lineshapes will not be distorted much.

From the point of view of TS and kinematics, the model discussed here shares the similar scenario with the  $D_1 D$  molecular state ansatz discussed in Refs. [30, 31, 34]. One different point is it incorporates the  $D_1 D$ ,  $D_1 D^*$  and  $D_2 D^*$  combinations in a single Lagrangian with the relative phase and coupling strength fixed in the heavy quark limit, which leads to most of the  $TH$  and  $HH$  cusp structures can be studied simultaneously in the same channel. Another crucial point is no matter whether the molecular state exist or not, it seems to be natural to suppose the coupled-channel effects, or the vacuum polarization effects, should exist physically.

This is not the whole story concerning the rescattering processes if we only take into account the  $THH$  loops. Since the experiments indicate the main decay channel of  $\psi(4160)$  is  $HH$ , we should also include the contribution from  $HHH$  loops, as illustrated in Fig. 1(C). But the threshold of  $HH$  is far away from the energy region discussed here, which does not favor the kinematic conditions of TS, and the coupling between  $\psi(nD)$  and  $HH$  is  $P$ -wave, which will also suppress the rescattering amplitude. To make it clear, we display the differential cross section for  $e^+e^- \rightarrow J/\psi\pi\pi$  in Fig. 3(a). At the center of mass energy around  $\sqrt{s} = 4.16$  GeV, if the rescattering occurs via  $THH$  loops, although it is not the favorable energy point for producing singularity, there is still a visible narrow cusp appeared around the  $DD^*$  threshold. But if the rescattering occurs via  $HHH$  loops, the cusp is nearly smeared and the lineshape becomes trivial, which is inconsistent with the result of CLEO-c [13]. This in another way supports the coupling between  $\psi(4160)$  and  $TH$  could be sizeable. We also studied the rescattering processes through  $\psi(nS)$  and  $SHH$  loops. As discussed in Ref. [31], since  $D_0$  and  $D'_1$  are too broad, if taking into account their width effects, the singularities will be smoothed and the amplitude will be lowered to some extent. We display one result in Fig. 3(b), where we have chosen  $\psi(4040)$  as the intermediate  $S$ -wave charmonia (another option is  $\psi(4415)$ ). It can be seen the cusps at  $D_0 D^*$ ,  $D'_1 D$ , and  $D'_1 D^*$  are smoothed by the broad width. This is just a simple estimation, since we only change the propagators in the loops to the Breit-Wigner functions, which may account for the contributions from higher order corrections. The real situation may be complicated. Although the lineshape behavior of  $HHH$  and  $SHH$  loops seems to be trivial, they can also provide some background for interference with  $THH$  loops.

### 3 Summary

In conclusion, we have discussed the lineshape behavior of the cross sections and distributions of  $e^+e^- \rightarrow J/\psi\pi\pi$ ,  $\psi'\pi\pi$  and  $h_c\pi\pi$ . The coupled-channel effects, especially that induced by the couplings between the  $D$ -wave charmonia and  $TH$  charmed mesons ( $THH$  loops), are highlighted. Because these leading order  $S$ -wave couplings will respect HQSS, and another important reason is the thresholds of  $TH$  are close to that of  $Y(4260)$  and  $Y(4360)$ . Taking  $\psi(4160)$  as the input  $\psi(nD)$ , we obtain some nontrivial lineshapes and cusps stay at the thresholds of  $TH$  and  $HH$ , which may have some underlying connections with the  $XYZ$  states observed around these thresholds. With a few theoretical uncertainties, the lineshape behavior is less model-dependent, and it indicates that these cusps are sensitive to the kinematics, that is because the TS of the  $THH$  loops has its favourable kinematic region. This can explain why  $Z_c(3900)/Z_c(3885)$  and  $Z_c(4020)/Z_c(4025)$  are observed in different processes and energy points. The  $\psi'\pi\pi$  channel can be taken as a direct prediction to check this scenario.

Our work just focus on the dipion transitions of the charmonia, as a qualitative guess, if the

coupled-channel effects induced by the  $P$ -wave charmed mesons are truly so important, maybe it can also compensate for the mass shift of charmonia sizeably.

## Acknowledgments

The author would like to thank S.L. Zhu, Q. Zhao, F.K. Guo and G. Li for helpful discussions. This work was supported in part by the China Postdoctoral Science Foundation under Grant No. 2013M530461, the National Natural Science Foundation of China under Grants No. 11075004 and No. 11021092, and the DFG and the NSFC through funds provided to the Sino-German CRC 110 "Symmetries and the Emergence of Structure in QCD."

## References

- [1] E. Eichten, K. Gottfried, T. Kinoshita, K. D. Lane and T. -M. Yan, Phys. Rev. D **17**, 3090 (1978) [Erratum-ibid. D **21**, 313 (1980)].
- [2] E. J. Eichten, K. Lane and C. Quigg, Phys. Rev. D **73**, 014014 (2006) [Erratum-ibid. D **73**, 079903 (2006)] [hep-ph/0511179].
- [3] M. R. Pennington and D. J. Wilson, Phys. Rev. D **76**, 077502 (2007) [arXiv:0704.3384 [hep-ph]].
- [4] T. Barnes and E. S. Swanson, Phys. Rev. C **77**, 055206 (2008) [arXiv:0711.2080 [hep-ph]].
- [5] B. -Q. Li, C. Meng and K. -T. Chao, Phys. Rev. D **80**, 014012 (2009) [arXiv:0904.4068 [hep-ph]].
- [6] F. -K. Guo, C. Hanhart, G. Li, U. -G. Meissner and Q. Zhao, Phys. Rev. D **83**, 034013 (2011) [arXiv:1008.3632 [hep-ph]].
- [7] Z. -Y. Zhou and Z. Xiao, arXiv:1309.1949 [hep-ph].
- [8] M. Ablikim *et al.* [BESIII Collaboration], Phys. Rev. Lett. **110**, 252001 (2013) [arXiv:1303.5949 [hep-ex]].
- [9] Z. Q. Liu *et al.* [Belle Collaboration], Phys. Rev. Lett. **110**, 252002 (2013) [arXiv:1304.0121 [hep-ex]].
- [10] M. Ablikim *et al.* [BESIII Collaboration], Phys. Rev. Lett. **111**, 242001 (2013) [arXiv:1309.1896 [hep-ex]].
- [11] M. Ablikim *et al.* [BESIII Collaboration], arXiv:1308.2760 [hep-ex].
- [12] M. Ablikim *et al.* [BESIII Collaboration], Phys. Rev. Lett. **112**, 022001 (2014) [arXiv:1310.1163 [hep-ex]].
- [13] T. Xiao, S. Dobbs, A. Tomaradze and K. K. Seth, Phys. Lett. B **727**, 366 (2013) [arXiv:1304.3036 [hep-ex]].
- [14] X. Liu, arXiv:1312.7408 [hep-ph].
- [15] S. L. Olsen, arXiv:1403.1254 [hep-ex].



- [16] X. Li and M. B. Voloshin, Phys. Rev. D **88**, 034012 (2013) [arXiv:1307.1072 [hep-ph]].
- [17] J. Beringer *et al.* [Particle Data Group Collaboration], Phys. Rev. D **86**, 010001 (2012).
- [18] M. Ablikim *et al.* [BES Collaboration], eConf C **070805**, 02 (2007) [Phys. Lett. B **660**, 315 (2008)] [arXiv:0705.4500 [hep-ex]].
- [19] X. H. Mo, C. Z. Yuan and P. Wang, Phys. Rev. D **82**, 077501 (2010) [arXiv:1007.0084 [hep-ex]].
- [20] R. Casalbuoni, A. Deandrea, N. Di Bartolomeo, R. Gatto, F. Feruglio and G. Nardulli, Phys. Lett. B **299**, 139 (1993) [hep-ph/9211248].
- [21] R. Casalbuoni, A. Deandrea, N. Di Bartolomeo, R. Gatto, F. Feruglio and G. Nardulli, Phys. Rept. **281**, 145 (1997) [hep-ph/9605342].
- [22] P. Colangelo, F. De Fazio and T. N. Pham, Phys. Rev. D **69**, 054023 (2004) [hep-ph/0310084].
- [23] T. Mehen and J. W. Powell, Phys. Rev. D **84**, 114013 (2011) [arXiv:1109.3479 [hep-ph]].
- [24] A. Margaryan and R. P. Springer, Phys. Rev. D **88**, 014017 (2013) [arXiv:1304.8101 [hep-ph]].
- [25] F. -K. Guo, C. Hanhart, U. -G. Meissner, Q. Wang and Q. Zhao, Phys. Lett. B **725**, 127 (2013) [arXiv:1306.3096 [hep-ph]].
- [26] Q. Wang, M. Cleven, F. -K. Guo, C. Hanhart, U. -G. Meissner, X. -G. Wu and Q. Zhao, Phys. Rev. D **89**, 034001 (2014) [arXiv:1309.4303 [hep-ph]].
- [27] P. V. Landshoff and S. B. Treiman, Phys. Rev. **127**, 649 (1962).
- [28] R. J. Eden, P. V. Landshoff, D. I. Olive and J. C. Polkinghorne, *The Ananytic S-Matrix*, Cambridge University Press 1966.
- [29] J. -J. Wu, X. -H. Liu, Q. Zhao and B. -S. Zou, Phys. Rev. Lett. **108**, 081803 (2012) [arXiv:1108.3772 [hep-ph]].
- [30] Q. Wang, C. Hanhart and Q. Zhao, Phys. Rev. Lett. **111**, 132003 (2013) [arXiv:1303.6355 [hep-ph]].
- [31] X. -H. Liu and G. Li, Phys. Rev. D **88**, 014013 (2013) [arXiv:1306.1384 [hep-ph]].
- [32] C. -Z. Yuan, arXiv:1312.6399 [hep-ex].
- [33] C. Z. Yuan *et al.* [Belle Collaboration], Phys. Rev. Lett. **99**, 182004 (2007) [arXiv:0707.2541 [hep-ex]].
- [34] M. Cleven, Q. Wang, F. -K. Guo, C. Hanhart, U. -G. Meissner and Q. Zhao, arXiv:1310.2190 [hep-ph].

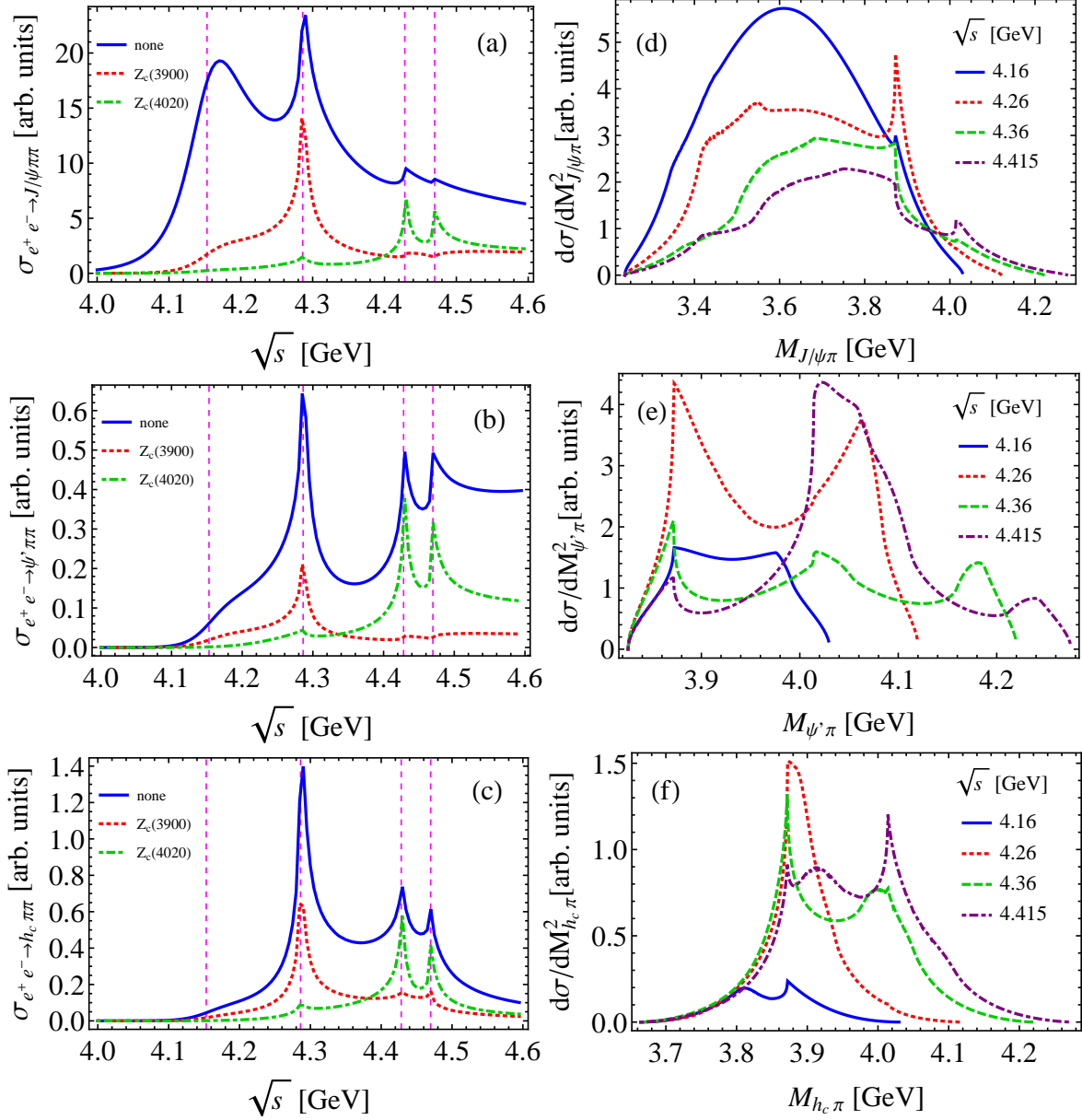


Figure 2: **Left):** Energy dependence of the cross section for  $e^+e^- \rightarrow$  (a)  $J/\psi\pi\pi$ , (b)  $\psi'\pi\pi$ , and (c)  $h_c\pi\pi$  via  $\psi(4160)$  and intermediate  $THH$  loops. The solid line is the result with only taking into account the contact interaction, the dotted and dot-dashed lines correspond to the result with plugging into  $Z_c(3900)$  and  $Z_c(4020)$  propagator respectively, and the magnitude of these lines has been rescaled to a similar level. The vertical lines (from left to right) indicate the mass of  $\psi(4160)$ , the thresholds of  $D_1D$ ,  $D_1D^*$  and  $D_2D^*$  respectively. **Right):** The corresponding invariant mass distributions of (d)  $J/\psi\pi$ , (e)  $\psi'\pi$ , and (f)  $h_c\pi$  at four center of mass energy points. Only the contact interactions are taking into account in  $THH$  loops.

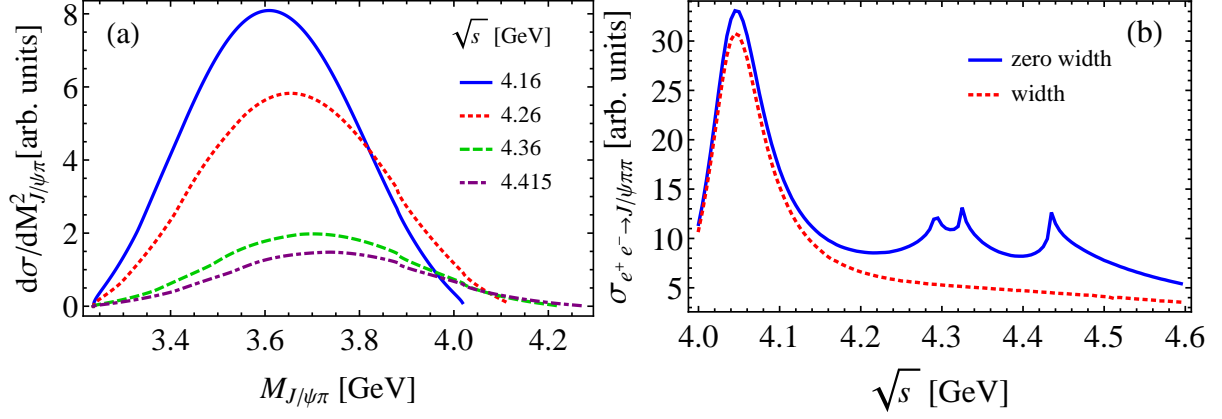


Figure 3: (a) Differential cross section for  $e^+e^- \rightarrow J/\psi\pi\pi$  via  $\psi(4160)$  and intermediate  $HHH$  loops. (b) Energy dependence of the cross section for  $e^+e^- \rightarrow J/\psi\pi\pi$  via  $\psi(4040)$  and intermediate  $SHH$  loops, where the solid and dotted line corresponds to the result with and without taking into account the broad width influence of  $D_0$  and  $D'_1$  respectively.